frontiers in
PHYSICS

ORIGINAL RESEARCH ARTICLE
published: 01 April 2014
doi: 10.3389/fphy.2014.00017

Orbital character and electron correlation effects on two- and three-dimensional Fermi surfaces in KFe_2As_2 revealed by angle-resolved photoemission spectroscopy

Teppei Yoshida[1,2]*†, Shin-Ichiro Ideta[1], Ichiro Nishi[1], Atsushi Fujimori[1,2], Ming Yi[3,4], Rob G. Moore[5], Sung-Kwan Mo[6], Donghui Lu[5], Zhi-Xun Shen[3,4], Zahid Hussain[6], Kunihiro Kihou[2,7], Parasharam M. Shirage[2,8], Hijiri Kito[2,8], Chul-Ho Lee[2,7], Akira Iyo[2,8], Hiroshi Eisaki[2,8] and Hisatomo Harima[2,9]

[1] Department of Physics, University of Tokyo, Bunkyo-ku, Tokyo, Japan
[2] JST, Transformative Research-Project on Iron Pnictides, Chiyoda, Tokyo, Japan
[3] Stanford Institute of Materials and Energy Sciences, SLAC National Accelerator Laboratory, Menlo Park, CA, USA
[4] Departments of Physics and Applied Physics, and Geballe Laboratory for Advanced Materials, Stanford University, Stanford, CA, USA
[5] Stanford Synchrotron Radiation Lightsource, SLAC National Accelerator Laboratory, Menlo Park, CA, USA
[6] Advanced Light Source, Lawrence Berkeley National Lab, Berkeley, CA, USA
[7] Energy Technology Research Institute, National Institute of Advanced Industrial Science and Technology, Tsukuba, Japan
[8] Electronics and Photonics Research Institute, National Institute of Advanced Industrial Science and Technology, Tsukuba, Japan
[9] Department of Physics, Kobe University, Kobe, Hyogo, Japan

Edited by:
Christos Panagopoulos, Nanyang Technological University, Singapore

Reviewed by:
Fengqi Song, Nanjing University, China
Anjan Soumyanarayanan, Massachusetts Institute of Technology, USA
Hong Ding, Chinese Academy of Sciences, China

****Correspondence:***
Teppei Yoshida, Graduate School of Human and Environmental Studies, Kyoto University, Yoshida-Nihonmatsu-cyo, Sakyo-ku, Kyoto 606-8501, Japan
e-mail: yoshida.teppei.8v@kyoto-u.ac.jp

†Present address:
Teppei Yoshida, Graduate School of Human and Environmental Studies, Kyoto University, Sakyo-ku, Kyoto, Japan

We have investigated orbital character and electron correlation effects on Fermi surfaces in the hole-overdoped iron pnictide superconductor KFe_2As_2, which shows a low T_c of ∼4 K, by angle-resolved photoemission spectroscopy. From the polarization-dependence of the ARPES spectra, we have determined the orbital character of each Fermi surface. Electron mass renormalization of each band is quantitatively consistent with de Haas-van Alphen results. The outer β and middle ζ Fermi surfaces show large renormalization factor of m^*/m_b ∼6–7, while the inner α Fermi surface has a smaller factor m^*/m_b ∼2. Middle hole Fermi surface ζ has strong three-dimensionality compared to other Fermi surfaces, indicating the d_{3z2-r2} orbital character, which may be related to the "octet-line nodes" recently observed by laser ARPES. The observed orbital-dependent mass renormalization would give constraints on the pairing mechanism with line nodes of this system.

Keywords: iron pnictide superconductor, angle-resolved photoemission spectroscopy, electron correlation

INTRODUCTION

In contrast to the *d*-wave superconducting gaps in the high-T_c cuprate superconductors, experimental results on most of the iron-pnictide superconductors have indicated that superconducting gaps are nodeless and on the entire Fermi surfaces (FSs) [1]. However, some of the iron pnictide superconductors show signatures of the nodes in the superconducting gaps. For example, thermal conductivity measurements of isovalent substituted system $BaFe_2(As_{1-x}P_x)_2$ [2] and the electron doped systems $Ba(Fe_{1-x}Co_x)_2As_2$ and $Ba(Fe_{1-x}Ni_x)_2As_2$ [3] in the superconducting state have shown signature of line nodes. According to the theories of spin fluctuation-mediated superconductivity, line nodes may appear when the pnictogen height becomes small [4, 5], the hole FS of d_{xy} character around the zone center disappears and nesting between hole and electron FSs becomes weakened. (Here, *x* and *y* are referred to the direction of the nearest neighbor Fe atoms). The hole FSs of these systems exhibit strong three-dimensionality [6–8], resulting in poor nesting between the hole and electron FSs.

The end member compound of K-doped $BaFe_2As_2$ (K-Ba122) system, KFe_2As_2, with a low T_c of ∼4 K [9] also shows signature of line nodes in penetration depth [10], thermal conductivity [11], and nuclear quadrupole resonance (NQR) measurements [12]. In fact, a recent laser angle-resolved photoemission (ARPES) study of KFe_2As_2 has revealed a superconducting gap with "octet-line nodes" on the middle hole FS (ζ FS) [13]. The observed nodes and a clear FS sheet dependence in the superconducting-gap size were well explained by a calculation with spin-fluctuation mechanism. However, the result is in strong contrast to the optimally doped K-Ba122 [14], while this is consistent with the evolution of the

gaps as a function of K doping [15]. Such a doping dependence in the superconducting gap may be related to the change in the FS topology. In going from the optimally [15, 16] to the overdoped region [17, 18] in K-Ba122 system, the electron pockets around the zone corner are replaced by small hole pockets surrounding the zone corner in a clover shape.

If the spin fluctuations are dominant in the pairing mechanism in KFe_2As_2, orbital dependent mass renormalization would be observed as a signature of spin fluctuations. So far, strong mass renormalization has been observed from the electronic specific heat coefficient γ as large as ~70–100 mJ/K^2 mol [12, 19]. Also, both the ARPES [18] and dHvA studies [20, 21] have indicated the enhancement of the electron masses compared to those predicted by the band-structure calculation.

Although three hole FSs (α, β, and ζ) have been clearly resolved in our previous ARPES study [18], the mass renormalization factor for each FS has not been clarified yet. In the present study, in order to reveal the orbital dependent mass renormalization in the iron-based superconductors, we have performed an ARPES study of KFe_2As_2 using high-quality single crystals. We have determined the orbital character of the FSs by polarization dependent measurements and have revealed strongly orbital dependent correlation effects.

EXPERIMENT AND BAND-STRUCTURE CALCULATION

ARPES measurements were performed at beamline 5–4 of Stanford Synchrotron Radiation Lightsource (SSRL) and at BL10.0.1 of Advanced Light Source (ALS). Scienta SES-R4000 electron analyzers and linearly polarized light were used at both beamlines. The typical energy resolutions were 10 meV at SSRL and 20 meV at ALS, respectively. Single crystals of KFe_2As_2 were grown from a self-flux method. Resistivity measurements on some of the grown crystals showed the residual resistivity ratio of ~600. Samples were cleaved *in situ* and measured at a temperature of 15 K in a pressure better than 5×10^{-11} Torr. We have performed the measurements at photon energies from $h\nu = 14$ to 40 eV. The in-plane (k_X, k_Y) and out-of-plane (k_Z) momentum are expressed in units of π/a and $2\pi/c$, respectively, where $a = 3.864$ Å and $c = 13.87$ Å. Here, the X and Y axes point toward the Fe-As bond direction, while the x and y axes are rotated by 45° from the X-Y coordination. The electronic band structure of KFe_2As_2 was calculated within the local density approximation (LDA) by using the full potential LAPW (FLAPW) method. We used the program codes TSPACE [22] and KANSAI-06. The experimental crystal structure [23] including the atomic position z_{As} of As (pnictogen height) was used for the calculation.

RESULTS AND DISCUSSION

Band dispersions for a cut along the diagonal of the two-dimensional Brillouin zone (BZ) taken with $h\nu = 25$ eV [18] and 30 eV are shown in **Figures 1A,B**. All the energy bands predicted by the calculation (**Figure 1C**) are observed. While three bands (α, β, and ζ) form hole FSs around the zone center, the ε band forms small hole FSs around the zone corner. The structure around 0.15 eV below E_F in **Figure 1A** is z^2 band shown in **Figure 1C**, which has a strong three dimensionality [18]. Another hole-like band crossing E_F near the zone center is a surface state [18].

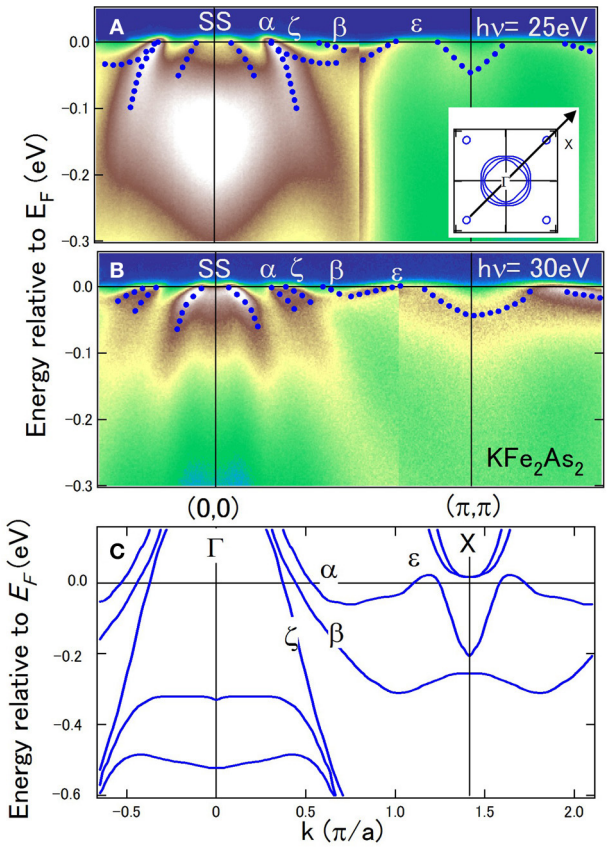

FIGURE 1 | Band dispersions of KFe_2As_2 in the zone diagonal direction. (A,B) ARPES spectra taken at $h\nu = 25$ eV [18] and 30 eV, respectively, corresponding to $k_z = 6.5$ and 7.0 ($2\pi/c$). SS denotes surface states. **(C)** Band dispersions predicted by band-structure calculation.

While the ζ band is nearly degenerated with the α band at $h\nu = 25$ eV, these bands are separated at $h\nu = 30$ eV, indicating three-dimensionality of the band dispersions. Note that the order of the α, β, and ζ bands from the zone center is different between theory and experimental data. We shall describe the present assignment of the band dispersions based on the matrix-element effect data as below.

FS mapping in k_X-k_Y plane is shown in **Figures 2A,B**. By assuming the inner potential $V_0 = 13.0$ eV (**Figures 2A,B**) approximately represent k_X-k_Y planes including the Γ and the Z point, respectively. All the three hole FSs around the center of the 2D BZ have been clearly resolved and small hole FSs appear around the BZ corner due to heavy hole doping. In **Figure 2B**, the surface states near the zone center form ridge-like structures extending to the k_X and k_Y directions, causing the peculiar cross-like intensity distribution [18]. We found that the middle hole FS (ζ) has different shape between the Γ and the Z point, indicating strong three dimensionality.

In **Figure 3**, we compare the FSs obtained by ARPES with the band-structure calculation. As seen in (**Figures 3A,B**), the sizes of the observed α and β FSs do not show appreciable change with k_z. On the other hand, the shape of the ζ FS significantly changes

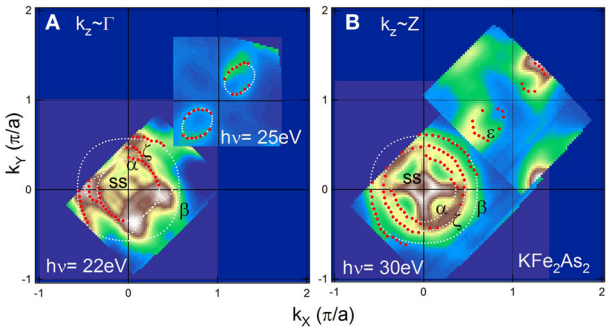

FIGURE 2 | FSs of KFe_2As_2 observed by ARPES. ARPES intensity at E_F mapped in the k_X-k_Y plane taken at different photon energies corresponding to $k_z \sim \Gamma$ **(A)** and $k_z \sim Z$ **(B)**. Red dots indicate k_F positions determined by the peak positions of momentum distribution curves (MDC's) and white dotted lines indicate FSs deduced from the k_F positions.

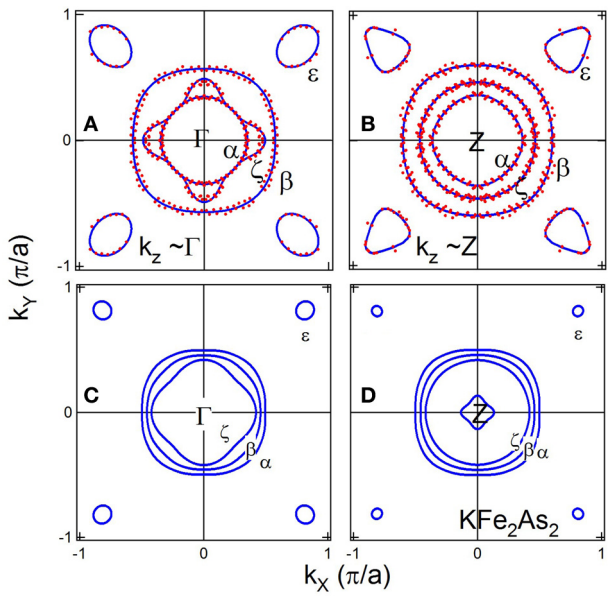

FIGURE 3 | Comparison of FSs obtained by ARPES and those predicted by band-structure calculation. (A,B) FSs determined by ARPES. k_F positions in **Figure 2** have been symmetrized in the first BZ. **(C,D)** FSs given by the band-structure calculation. A small FS around the Z point comes from a three-dimensional d_{z2} band.

between $k_z \sim \Gamma$ and Z. While the ζ FS has a diamond-like cross-section for $k_z \sim \Gamma$ and is nearly degenerate with the α FS in the zone diagonal direction, it has a circular cross-section for $k_z \sim$ Z. Such a change is seen in the inner-most calculated hole FS in **Figures 3C,D**.

In order to determine the orbital character of the FSs, we have investigated the polarization dependence of the ARPES intensity as shown in **Figure 4**. FS mapping shown in (**Figures 4A,B**) indicates clear polarization dependence in the intensity distribution for each FS. We have simulated the intensity distribution by using the following assumptions. Based on the result of the band-structure calculation, we assume that three orbitals *xy*, *yz*, and *zx*

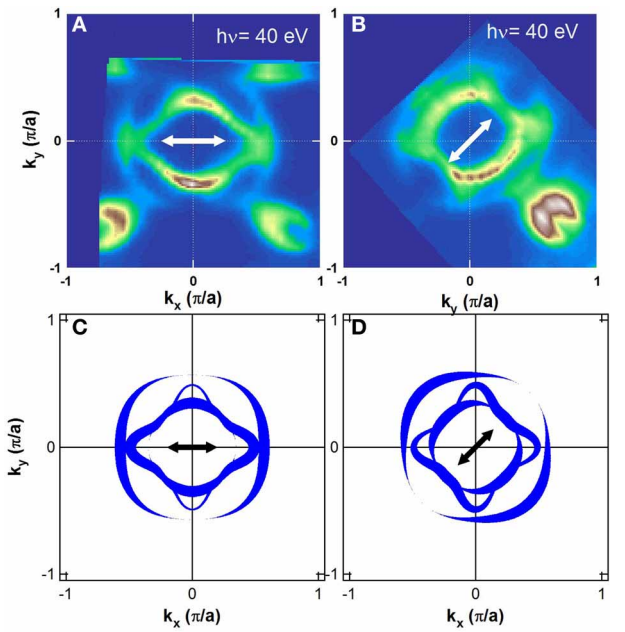

FIGURE 4 | Polarization dependence of the FS mapping for KFe_2As_2. (A,B) Measured ARPES intensity at E_F in the k_X-k_Y plane taken at $h\nu = 40$ eV ($k_z \sim \Gamma$). Electric vectors are shown by arrows. **(C,D)** Simulation of the ARPES intensity distribution corresponding to **(A,B)**. Shapes of FSs have been taken from **Figure 2**. By assuming certain orbital character for each FS, intensity distribution has been simulated and is shown by thickness of the curves (For details, see the text).

constitute the FSs. We refer to the three band as *xy*, *yz*, and *zx* band according to the orbital character of the band with momentum in the zone diagonal k_x (// $k_X + k_Y$) direction. Using the angle θ around the Γ point, the orbital character of the *xy*, *zx*, and *yz* band can be approximately expressed by $|xy>$, $\cos\theta\ |zx> + \sin\theta\ |yz>$ and $-\sin\theta\ |zx> + \cos\theta\ |yz>$, respectively. By assuming the dipole approximation of the transition matrix element $|<i|\boldsymbol{\varepsilon}\cdot\boldsymbol{r}|f>|^2$, where $|i>$, $|f>$, and $\boldsymbol{\varepsilon}$ are the initial state, the final state, and the polarization vector, respectively, one can predict the intensity distribution. For example, when $|i>=|xy>$, $\boldsymbol{\varepsilon}$ //x and $|f>$ is a wave function of a free electron, the transition matrix element $|<i|\boldsymbol{\varepsilon}\cdot\mathbf{r}|f>|^2$ is proportional to k_y^2 in the lowest order in $\boldsymbol{k}$.

Figures 4C,D are the results of the intensity simulations of the FSs whose shapes have been determined by the present experimental data. Here, we assign the inner, middle, and outer FSs to the *yz*, *xz*, and *xy*-band, respectively, so that we can reproduce the experimental intensity distribution. This assignment of the orbital character is different from the band-structure calculation where the inner, middle, and outer FSs have *xz*, *xy*, and *yz* orbital character, respectively. However, the present ARPES result is consistent with the previous ARPES result of Co-Ba122 [24] and the theoretical prediction of LDA+DMFT [25], which indicate the energy inversion of the *xy* and *yz*/*xz* bands due to orbital-dependent correlation effect. This trend is also consistent with an ARPES result of LiFeAs [26]. That is, the *xy* band in most strongly affected by electron correlation and is shifted upward relative to the other bands.

Another discrepancy from the band-structure calculation is the inversion of the *yz* and *xz* bands in the k_X (k_Y) direction. In the result of the band-structure calculation, the inner FS has *xz* character (in the k_X direction) with rounded-square shape around the Γ point and becomes circular around the *Z* point because of hybridization with the z^2 orbital. In the present ARPES result, such a character has been observed in the middle ζ FS. According to the angular-dependent magnetoresistance oscillations, such a rounded-square FS is also bigger than a circular hole FS [27]. The observed inversion of the *xz*, *yz* bands is consistent with the ARPES result of Co-Ba122 [24] and the LDA+DMFT calculation for KFe_2As_2 [25].

In the dHvA study, the sizes of the hole FSs are found to be smaller than those predicted by band-structure calculations [9]. We have determined the cross-sectional area of the FSs as listed in **Table 1** together with those of the dHvA measurements and the band-structure calculation. The cross-sectional areas for the α and ζ FSs observed by ARPES are close to those obtained by the dHvA result and are smaller than the band-structure calculation. On the other hand, the area of the β and ε FSs determined by ARPES are much larger than the calculation results. The total hole count from the observed FSs yields the hole FS volume of 61% of the BZ, indicating a deviation from the value of 50% expected from the chemical composition, because most of the FSs observed by ARPES are nearly 10–20% larger than those observed by dHvA. The deviation of the FS volume implies that there is excess hole doping of 0.11 per Fe atom at the sample surface. Nevertheless, the surface effect is not so serious as those in 1111 system where excess 0.5–0.6 holes per Fe are doped [28], and one can still discuss mass renormalization from the present result.

The effective masses determined by ARPES are compared with those derived from the dHvA measurements and the band-structure calculation in **Table 1**. For all the FSs, the effective mass ratio m^*/m_e, where m_e is the free electron mass, determined by ARPES is in good agreement with those obtained by dHvA. For the hole FSs around the zone center, the outer β and middle ζ FSs show large renormalization factor of m^*/m_b ∼6–7, while the inner α FS has a smaller factor m^*/m_b ∼2. The strong mass enhancement for the β and ζ band may be due to the fact that the orbitals are directed to the Fe-As bond direction, causing the enhancement of electron correlation effects. Particularly, according to LDA+DMFT calculation [19, 25], a larger mass renormalization is expected in the *xy* band than those of the *yz*/*xz* bands. Thus, the observed mass enhancement factors indicate moderate to strong electron correlation. From the effective masses m^* listed in **Table 1**, the electronic specific heat coefficient γ is calculated to be γ ∼90 mJ/molK^2, which is close to γ = 103 mJ/molK^2 estimated from specific heat measurements [19].

The penetration depth [10] and thermal conductivity [11] measurements of KFe_2As_2 suggest that line nodes exist in the superconducting gap. Particularly, recent thermal conductivity result [29] has been interpreted based on the *d*-wave symmetry in KFe_2As_2. Because the small hole FSs around the zone corner are too small to account for the linear temperature dependence of the superfluid density [10], the node should be on the zone-centered hole FSs. In fact, the "octet-node" has been observed in the ζ hole FS by the laser ARPES study [13]. Based on the spin-fluctuation-mediated model calculation, the octet node can be interpreted as vertical nodes with A_{1g} gap symmetry, which originates from the $3z^2$-r^2 orbital character of the ζ hole FS. Such octet nodes may not contradict with the observation of the node on the small hole pockets in $Ba_{0.1}K_{0.9}Fe_2As_2$ [30], if the vertical nodal line with A_{1g} gap symmetry rapidly shifts in the momentum space with hole doping. On the other hand, a small-angle neutron scattering measurement on KFe_2As_2 has suggested the existence of a horizontal node [31]. One should note that both the vertical and horizontal nodes [32–34] can be realized in the region of the FS with $3z^2$-r^2 orbital character. In the present work, we revealed that the ζ FS has a strong three-dimensionality compared to the other FSs, implying a significant amount of the $3z^2$-r^2 character in the ζ FS.

CONCLUSION

We have performed an ARPES study of KFe_2As_2 to investigate orbital-dependent correlation effects. The orbital character of each FS is determined by the polarization dependence of the ARPES intensity. The value of the electron mass renormalization for each band indicates orbital-dependent correlation effects and is consistent with the dHvA result [20, 21] and the DMFT calculation [25]. Particularly, the β and ζ FS show large mass enhancement of m^*/m_b ∼ 6–7. Only the middle hole FS ζ shows a clear three-dimensionality, suggestive of $3z^2$-r^2 orbital character, which may be related to the "octet nodes" [13]. The precise

Table 1 | Cross-sectional areas and effective masses of FSs of KFe_2As_2 determined by ARPES and dHvA experiment [20, 21].

		Area			m^*/m_e (m^*/m_b)		
FS	k_z	**ARPES**	**dHvA**	**LDA**	**ARPES**	**dHvA**	**LDA**
α	Γ	9.1	8.2	20.8	5.1 (2.0)	6.0 (2.3)	2.6
	Z	9.8	8.6	21.6	6.6 (2.3)	6.5 (2.2)	2.9
ζ	Γ	12.2	10.3	12.2	11.0 (7.9)	8.5 (6.1)	1.4
	Z	17.0	15.7	13.8	17.7 (7.4)	18 (7.5)	2.4
β	Γ	27.3	25.6	16.7	16.3 (6.3)	19 (7.3)	2.6
	Z	30.0		17.4	17.9 (6.9)		2.6
ε	Γ	2.1	0.86	0.11	5.6 (18.7)	6.0 (20)	0.3
	Z	2.1	1.29	0.36	4.1 (13.7)	7.2 (24)	0.3

The areas are expressed as a percentage of the area of the 2D BZ. m_e and m_b are the free-electron and band masses, respectively.

determination of the orbital dependent mass renormalization in the present study would give constraint on the pairing mechanism with line nodes.

ACKNOWLEDGMENTS

We are grateful to K. Kuroki, R. Arita, H. Fukazawa, T. Terashima and M. Kimata for enlightening discussions. Thanks are also due to K. Haule for showing us the result of LDA-DMFT calculations prior to publication. This work was supported by the Japan-China-Korea A3 Foresight Program and a Grant-in-Aid for Young Scientist (B) (22740221) from the Japan Society for the Promotion of Science. SSRL is operated by the US DOE Office of Basic Energy Science Divisions of Chemical Sciences and Material Sciences. ALS is supported by the U.S. DOE (Contract No. DE-AC02-05CH11231).

REFERENCES

1. Ding H, Richard P, Nakayama K, Sugawara K, Arakane T, Sekiba Y, et al. Observation of Fermi-surface-dependent nodeless superconducting gaps in $Ba_{0.6}K_{0.4}Fe_2As_2$. *Europhys Lett.* (2008) **83**:47001. doi: 10.1209/0295-5075/83/47001
2. Hashimoto K, Yamashita M, Kasahara S, Senshu Y, Nakata N, Tonegawa S, et al. Line nodes in the energy gap of superconducting $BaFe_2(As_{1-x}P_x)_2$ single crystals as seen via penetration depth and thermal conductivity. *Phys Rev B* (2010) **81**:220501. doi: 10.1103/PhysRevB.81.220501
3. Reid JP, Tanatar MA, Luo XG, Shakeripour H, Doiron-Leyraud N, Ni N, et al. Nodes in the gap structure of the iron arsenide superconductor $Ba(Fe_{1-x}Co_x)_2As_2$ from *c*-axis heat transport measurements. *Phys Rev B* (2010) **82**:064501. doi: 10.1103/PhysRevB.82.064501
4. Kuroki K, Usui H, Onari S, Arita R, Aoki H. Pnictogen height as a possible switch between high-T_c nodeless and low-T_c nodal pairings in the iron-based superconductors. *Phys. Rev. B* (2009) **79**:224511. doi: 10.1103/PhysRevB.79.224511
5. Ikeda H, Arita R, Kuneš J. Phase diagram and gap anisotropy in iron-pnictide superconductors. *Phys Rev B* (2010) **81**:054502. doi: 10.1103/PhysRevB.81.054502
6. Yoshida T, Nishi I, Ideta S, Fujimori A, Kubota M, Ono K, et al. Two-Dimensional and Three-Dimensional Fermi surfaces of superconducting $BaFe_2(As_{1-x}P_x)_2$ and their nesting properties revealed by angle-resolved photoemission spectroscopy. *Phys Rev Lett.* (2011) **106**:117001. doi: 10.1103/PhysRevLett.106.117001
7. Malaeb W, Yoshida T, Fujimori A, Kubota M, Ono K, Kihou K, et al. Three-Dimensional electronic structure of superconducting iron pnictides observed by angle-resolved photoemission spectroscopy. *J Phys Soc Jpn.* (2009) **78**:123706. doi: 10.1143/JPSJ.78.123706
8. Vilmercati P, Fedorov A, Vobornik I, Manju U, Panaccione G, Goldoni A, et al. Evidence for three-dimensional Fermi-surface topology of the layered electron-doped iron superconductor $Ba(Fe_{1-x}Co_x)_2As_2$. *Phys Rev B* (2009) **79**:220503. doi: 10.1103/PhysRevB.79.220503
9. Terashima T, Kimata M, Satsukawa H, Harada A, Hazama K, Uji S, et al. Resistivity and upper critical field in KFe_2As_2 single crystals. *J Phys Soc Jpn.* (2009) **78**:063702. doi: 10.1143/JPSJ.78.063702
10. Hashimoto K, Serafin A, Tonegawa S, Katsumata R, Okazaki R, Saito T, et al. Evidence for superconducting gap nodes in the zone-centered hole bands of KFe_2As_2 from magnetic penetration-depth measurements. *Phys Rev B* (2010) **82**:014526. doi: 10.1103/PhysRevB.82.014526
11. Dong JK, Zhou SY, Guan TY, Zhang H, Dai YF, Qiu X, et al. Quantum criticality and nodal superconductivity in the FeAs-Based superconductor KFe_2As_2. *Phys Rev Lett.* (2010) **104**:087005. doi: 10.1103/PhysRevLett.104.087005
12. Fukazawa H, Yamada Y, Kondo K, Saito T, Kohori Y, Kuga K, et al. Possible multiple gap superconductivity with line nodes in heavily hole-doped superconductor KFe_2As_2 studied by 75As nuclear quadrupole resonance and specific heat. *J Phys Soc Jpn.* (2009) **78**:083712. doi: 10.1143/JPSJ.78.083712
13. Okazaki K, Ota Y, Kotani Y, Malaeb W, Ishida Y, Shimojima T, et al. Octet-Line node structure of superconducting order parameter in KFe_2As_2. *Science* (2012) **337**:1314. doi: 10.1126/science.1222793
14. Shimojima T, Sakaguchi F, Ishizaka K, Ishida Y, Kiss T, Okawa M, et al. Orbital-Independent superconducting gaps in iron pnictides. *Science* (2011) **332**:564. doi: 10.1126/science.1202150
15. Malaeb W, Shimojima T, Ishida Y, Okazaki K, Ota Y, Ohgushi K, et al. Abrupt change in the energy gap of superconducting $Ba_{1-x}K_xFe_2As_2$ single crystals with hole doping. *Phys Rev B* (2012) **86**:165117. doi: 10.1103/PhysRevB.86.165117
16. Zabolotnyy VB, Inosov DS, Evtushinsky DV, Koitzsch A, Kordyuk AA, Sun GL, et al. (π, π) electronic order in iron arsenide superconductors. *Nature* (2009) **457**:569. doi: 10.1038/nature07714
17. Sato T, Nakayama K, Sekiba Y, Richard P, Xu YM, Souma S, et al. Band structure and Fermi surface of an extremely overdoped iron-based superconductor KFe_2As_2. *Phys Rev Lett.* (2009) **103**:047002. doi: 10.1103/PhysRevLett.103.047002
18. Yoshida T, Nishi I, Fujimori A, Yi M, Moore R, Lu DH, et al. Fermi surfaces and quasi-particle band dispersions of the iron pnictides superconductor KFe_2As_2 observed by angle-resolved photoemission spectroscopy. *J Phys Chem Solids* (2011) **72**:465. doi: 10.1016/j.jpcs.2010.10.064
19. Hardy F, Böhmer AE, Aoki D, Burger P, Wolf T, Schweiss P, et al. Evidence of strong correlations and coherence-incoherence crossover in the iron pnictide superconductor KFe_2As_2. *Phys Rev Lett.* (2013) **111**:027002. doi: 10.1103/PhysRevLett.111.027002
20. Terashima T, Kimata M, Kurita N, Satsukawa H, Harada A, Hazama K, et al. Fermi surface and mass enhancement in KFe_2As_2 from de Haas–van Alphen effect measurements. *J Phys Soc Jpn.* (2010) **79**:053702. doi: 10.1143/jpsj.79.053702
21. Terashima T, Kurita N, Kimata M, Tomioka M, Tsuchiya S, Imai M, et al. Fermi surface in KFe_2As_2 determined via de Haas–van Alphen oscillation measurements. *Phys Rev B* (2013) **87**:224512. doi: 10.1103/PhysRevB.87.224512
22. Yanase A. *FORTRAN Program for Space Group.* 1st ed. Shokabo, Tokyo (1985).
23. Rozsa S, Schuster HUZ. Crystal-structure of KFe_2As_2, KCo_2As_2, KRh_2As_2 and KRh_2P_2. *Naturforsch B* (1981) **36**:1668.
24. Zhang Y, Chen F, He C, Zhou B, Xie BP, Fang C, et al. Orbital characters of bands in the iron-based superconductor $BaFe_{1.85}Co_{0.15}As_2$. *Phys Rev B* (2011) **83**:054510. doi: 10.1103/PhysRevB.83.054510
25. Yin ZP, Haule K, Kotliar G. Kinetic frustration and the nature of the magnetic and paramagnetic states in iron pnictides and iron chalcogenides. *Nat Mater.* (2011) **10**:932. doi: 10.1038/nmat3120
26. Lee G, Ji HS, Kim Y, Kim C, Haule K, Kotliar G, et al. Orbital selective fermi surface shifts and mechanism of high T_c superconductivity in correlated AFeAs (A=Li, Na). *Phys Rev Lett.* (2012) **109**:177001. doi: 10.1103/PhysRevLett.109.177001
27. Kimata M, Terashima T, Kurita N, Satsukawa H, Harada A, Kodama K, et al. Quasi-Two-Dimensional fermi surfaces and coherent interlayer transport in KFe_2As_2. *Phys Rev Lett.* (2010) **105**:246403. doi: 10.1103/PhysRevLett.105.246403
28. Nishi I, Ishikado M, Ideta S, Malaeb W, Yoshida T, Fujimori A, et al. Angle-resolved photoemission spectroscopy study of $PrFeAsO_{0.7}$: comparison with LaFePO. *Phys Rev B* (2011) **84**:014504. doi: 10.1103/PhysRevB.84.014504
29. Reid J-Ph, Tanatar MA, Juneau-Fecteau A, Gordon RT, René de Cotret S, Doiron-Leyraud N, et al. Universal heat conduction in the iron arsenide superconductor KFe_2As_2: evidence of a *d*-Wave State. *Phys Rev Lett.* (2012) **109**:087001. doi: 10.1103/PhysRevLett.109.087001
30. Xu N, Richard P, Shi X, van Roekeghem A, Qian T, Razzoli E, et al. Possible nodal superconducting gap and Lifshitz transition in heavily hole-doped $Ba_{0.1}K_{0.9}Fe_2As_2$. *Phys Rev B* (2013) **88**:220508. doi: 10.1103/PhysRevB.88.220508
31. Kawano-Furukawa H, Bowell CJ, White JS, Heslop RW, Cameron AS, Forgan EM, et al. Gap in KFe_2As_2 studied by small-angle neutron scattering observations of the magnetic vortex lattice. *Phys Rev B* (2011) **84**: 024507. doi: 10.1103/PhysRevB.84.024507
32. Graser S, Kemper AF, Maier TA, Cheng HP, Hirschfeld PJ, Scalapino DJ. Spin fluctuations and superconductivity in a three-dimensional tight-binding model for $BaFe_2As_2$. *Phys Rev B* (2010) **81**:214503. doi: 10.1103/PhysRevB.81.214503
33. Suzuki K, Usui H, Kuroki K. Possible Three-Dimensional nodes in the $s\pm$ superconducting gap of $BaFe_2(As_{1-x}P_x)_2$. *J Phys Soc Jpn.* (2011) **80**:013710. doi: 10.1143/JPSJ.80.013710

34. Suzuki K, Usui H, Kuroki K. Spin fluctuations and unconventional pairing in KFe_2As_2. *Phys Rev B* (2011) **84**:144514. doi: 10.1103/PhysRevB.84.144514

Conflict of Interest Statement: The authors declare that the research was conducted in the absence of any commercial or financial relationships that could be construed as a potential conflict of interest.

Received: 22 December 2013; accepted: 05 March 2014; published online: 01 April 2014.
*Citation: Yoshida T, Ideta S-I, Nishi I, Fujimori A, Yi M, Moore RG, Mo S-K, Lu D, Shen Z-X, Hussain Z, Kihou K, Shirage PM, Kito H, Lee C-H, Iyo A, Eisaki H and Harima H (2014) Orbital character and electron correlation effects on two- and three-dimensional Fermi surfaces in KFe_2As_2 revealed by angle-resolved photoemission spectroscopy. Front. Physics **2**:17. doi: 10.3389/fphy.2014.00017*
This article was submitted to Condensed Matter Physics, a section of the journal Frontiers in Physics.